Int. J. Environ. Sci. Technol. (2015) 12:1223–1234
DOI 10.1007/s13762-013-0492-9

ORIGINAL PAPER

Removal of industrial pollutant (Reactive Orange 122 dye) using environment-friendly sorbent *Trapa bispinosa's* peel and fruit

M. Saeed · R. Nadeem · M. Yousaf

Received: 14 May 2013 / Revised: 27 November 2013 / Accepted: 21 December 2013 / Published online: 24 January 2014

Abstract Removal of color water pollution due to Reactive Orange 122 dye was investigated using an inexpensive, locally available *Trapa bispinosa*. Fruit and peels of *T. bispinosa* biomass was used for this context in free, polyvinyl alcohol immobilized and chemically (H_2O_2) treated form. The aftermath of operational parameters such as pH (1.0–6.0), dye initial concentration (10–350 mg L^{-1}) and contact time (0–1,440 min) was investigated for maximum removal of dye from aqueous solution. Analysis was performed on UV–Vis spectrophotometer before and after sorption phenomenon. Maximum uptake was observed at pH 1.0. Highest q (mg g^{-1}) was shown by H_2O_2-treated *T. bispinosa* fruit (46.36) and H_2O_2-treated *T. bispinosa* fruit beads (43.00). The sorption rate was rapid in first 30 min, and equilibrium was established in 120 min. It was observed that best model was pseudo-second order, with correlation coefficient in the range of 0.987–1.00. Langmuir model effectively described the sorption data with X_m and R^2 that were in good agreement with experimental q (mg g^{-1}). Regeneration of the sorbent was done by performing desorption cycles, which made the method environment-friendly and more economical. Surface morphology and elemental analysis of a sample were carried out.

Keywords *Trapa bispinosa* · Reactive Orange 122 · Langmuir model · SEM · EDX · Desorption

M. Saeed · R. Nadeem (✉) · M. Yousaf
Department of Chemistry and Biochemistry, University of Agriculture, Faisalabad 38040, Pakistan
e-mail: raziyaanalyst@yahoo.com

Introduction

Increasing industrialization and urbanization lead to contamination of water resources. Control on water pollution is one of the prime concerns of science today, and dye pollutants are considered as hazardous dilemma (Zhang 2013). For coloration of products, dyes are used in various textile industries such as pulp, paper, leather, pharmaceuticals, textiles, paint, tanneries, plastics, rubber, food processing, cosmetics, electroplating and in wet process such as printing, bleaching, scouring, dyeing, mercerizing and final finishing (Ponnusami et al. 2007; Iqbal et al. 2011; Sadaf and Bhatti 2011). The color attained by water streams, such as lakes or rivers, emerging from mentioned industries is highly undesirable and visible even at minor concentration. More than 15 % of the used dyestuffs are drained out in the water process. As a consequence, unclearness and turbidity impede sunlight penetration, which leads to decline in photosynthetic activity and further inhibits desirable growth of aquatic life essential for maintenance of symbiotic process and self-purification. High toxicity of colored effluents to aquatic biota is reported. Moreover, their dangerous, genotoxic, mutagenic and carcinogenic effect to aquatic life has been evaluated (Yesilada et al. 2003; Aksu and Agatay 2006; Safa and Bhatti 2011).

More than 100,000 structurally dissimilar dyes are being manufactured, and annual production is 7×10^5 tonnes (Aksu and Balibek 2010; Mao et al. 2010). On the basis of

dyeing process, textile dyes are classified as basic dyes, acid dyes, reactive dyes, disperse dyes, direct dyes and vat dyes (Murugesan et al. 2006). Usage of reactive dyes is predominant due to their binding capacity through covalent bond with textile fibers and their affirmative individuality such as water-fasting, color brightness and simple appliance techniques (Fernandez et al. 2008; Ju et al. 2008; Deniz and Karaman 2011). Azo-based chromophores of reactive dyes show compatibility with a verity of reactive groups such as difluorochloropyrimidine vinyl sulfone, trichloropyrimidine and chlorotriazine (Vijayaraghavan and Yun 2007; Junxiong et al. 2009; Sadettin and Donmez 2006; Handan 2011). Complex aromatic nature of reactive dyes causes stability to heat, light, oxidizing agent and resistant to fading and biodegradability. So, effluent containing dyes are hardly decolorized to conventional biological, physicochemical processes, such as flocculation, coagulation, dilution, catalysis, ultrafiltration, adsorption, chemical precipitation, ozonation, ion-exchange, chemical and complex oxidation. These treatments are difficult, ineffective and not eco-friendly. In fact, 90 % of reactive dyes after activated sludge process remain unaffected (Mondal 2008; Gadd 2009; Safa and Bhatti 2011).

Biosorption, a physicochemical phenomenon, is an alternative, attractive, convenient to operate and posses numerous inherent benefits, such as simplicity of design, abundant in nature, cheap, efficient, possible recycle of biosorbents, wide range of operation conditions. Mostly, biosorbents have revealed valuable because of their good binding capability toward various dye groups (Crini 2006; Ju et al. 2008; Vijayaraghavan et al. 2008). Sorption mechanisms involve adsorption, chelation, ion-exchange, complexation and binding behavior depends upon pollutant's chemical nature, biosorbent's type and conditions such as ionic strength, temperature and pH. Many agricultural wastes have been used as biosorbent for decolonization and detoxification of water stream. Modifications or pretreatments of the biomaterial may amplify the surface area of the biosorbent and improved the uptake of pollutant from the solution (Oei et al. 2009; Bhatti et al. 2010).

Immobilization of biosorbent is being practiced due to several benefits such as ease of reuse, enhancing mechanical strength, constancy of particle and minimum flocculation. Various researchers have used polymeric matrix for immobilization of biosorbent, for example, in 2003, Bai and Abraham and, in 2012, Asgher and Bhatti used polyacrylamide and alginate. In 2003, Beolchini et al. used polysulfone. Polyvinyl alcohol (PVA) is non-toxic polymer, less costly and efficient polymer (Bai and Abraham 2003; Beolchini et al. 2003; Asgher and Bhatti 2012).

An extensive search of the literature reveals no reports on the sorption activity of *Trapa bispinosa*'s fruit and peel (TBF, TBP). Its fruit and peel can be employed as a cheap adsorbent. *T. bispinosa* is an edible aquatic angiosperm locally known as "Singhara" and water chestnuts. In this study, biosorbent was pretreated with oxidizing agent (H_2O_2). The present work was carried out to explore the effect and comparison of immobilized and free form of *Trapa bispinosa*'s fruit and peel. Moreover, the outcome of dye initial concentration, pH and contact time was also investigated. The research work was carried out in Bioanalytical Chemistry Lab, Department of Chemistry and Biochemistry, University of Agriculture, Faisalabad, in 2012.

Materials and methods

Preparation and modification of *T. bispinosa*'s peel and fruit

Trapa bispinosa's peel and fruit (TBP and TBF) were taken from different areas of Faisalabad, Pakistan. TBP and TBF washed with water and dried out in the sunlight. Then ground using food processor (Moulinex, France) and sieved through Octagon siever (OCT-DIGITAL 4527-01) to particles of 0.25 mm. Fine powder of TBP and TBF was divided into two portions. One portion was saved as free biomass, and second portion was subjected to pretreatment with 0.1 N of oxidizing agent (H_2O_2) and shake them in orbital shaker (OCT-DIGITAL4527-01) at 100 rpm for 24 h. Samples were dried in oven for 24 h at 80 °C.

Immobilization of sorbent

Ten gram PVA (10 % W/V) and 2 g sorbent mix in 100 mL water by heating. One gram sorbent and 1 g Na-alginate (1 % W/V) in 100 mL water by heating. Both mixtures were mixed together by heating. Added the mixture in 1,000 mL burette and dropped into 50 % sodium nitrate (W/V) and 1 % calcium chloride (W/V) solution mixture for the formation of immobilized beads of sorbent. The beads were washed with water and kept at cool place.

Preparation of aqueous reactive dyes solution

In the present work, reactive dye, Orange C2RL 122 (RO 122) was taken from Sandal Dyestuff Industry, Faisalabad.

RO 122 is anionic type having MCT/VS reactive groups. Structure of RO 122 dye is given in Fig. 1a. Stock solution of dye was prepared by dissolving 1 g of dye in 1,000 mL of distilled water. Standard curves of dye solution for λ_{max} were investigated by the absorbance measurement through UV–Vis spectrophotometer (PG-T 60 Spectrophotometer). RO 122 showed maximum absorbance at 500 nm as shown in Fig. 1b.

Batch sorption protocol

In the batch sorption studies, the 250-mL conical flasks containing 0.1 g sorbent in 50 mL of dye solution of adjusted pH (1–6), 0–1,440 min contact time and different concentrations (10–350 mg L^{-1}) of Reactive Orange C2RL 122 were shaken in orbital shaker at 100 rpm to evaluate the effect of these parameters. The experiments were performed at room temperature. The sorbent was removed by centrifugation at 600 rpm for 5 min, and absorbance was measured by spectrophotometer (PG-T 60 Spectrophotometer). Blank solutions were also run with same conditions except the addition of sorbent material.

Desorption

Desorption was carried out with adsorbate-loaded biosorbents obtained from batch processes, in which the adsorbate solutions (50 mg L^{-1}) were treated with optimum dosage of adsorbents for optimum contact time. The TBF and TBF beads washed smoothly with water for the removal of unsorbed dye. After washing, biosorbents were dissolved in flask containing 50 mL 0.01 N NaOH as a desorption agent. Sorption and desorption were carried out up to three cycles.

Calculations

The dye sorption capacity of biosorbents was calculated from the following equation (Seey and Kassim 2012):

$$q_e = \frac{(C_i - C_e)}{M} \times V \quad (1)$$

The % sorption was calculated from the following equation:

$$\%\,\text{sorption} = \frac{C_i - C_e}{C_i} \times 100 \quad (2)$$

where q_e (mg g^{-1}) is the adsorption capacity of the biosorbent at any time, C_i and C_e are the initial and

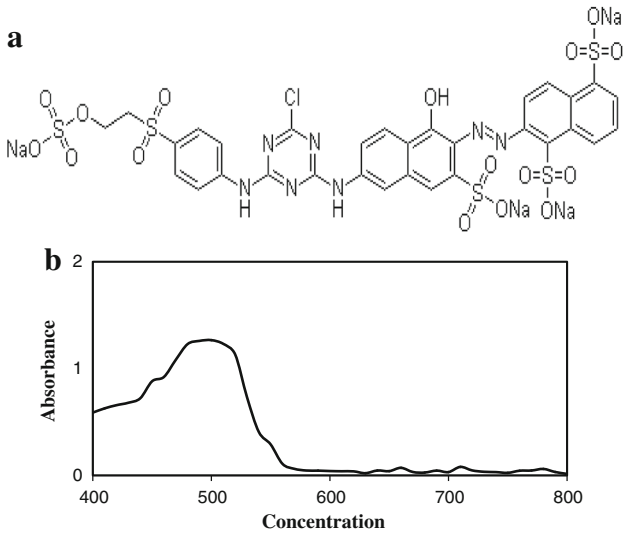

Fig. 1 **a** Structure of Reactive Orange 122 (RO 122) and **b** λ_{max} plot for RO 122

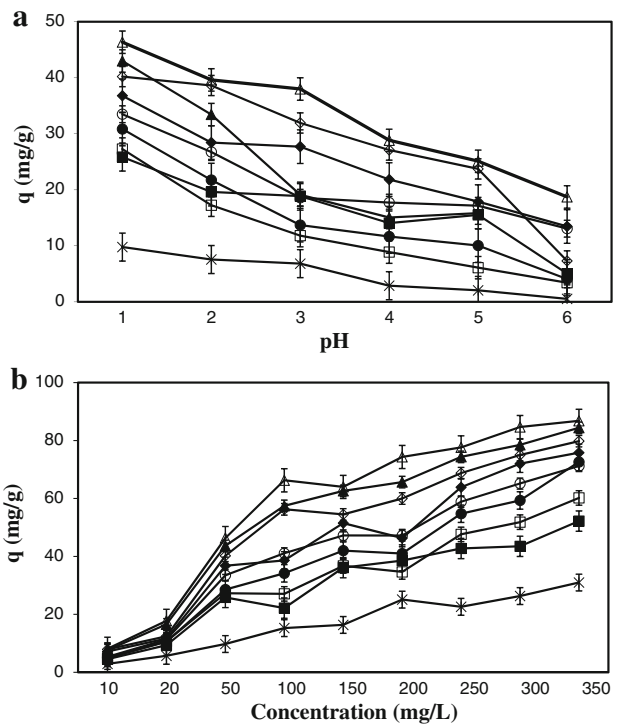

Fig. 2 **a** Effect of pH and **b** effect of concentration on the sorption of Reactive Orange 122 by *T. bispinosa*'s peel and fruit. *Times symbol* PVA-alginate, *opened square* TBP, *filled square* TBP beads, *opened diamond* TBF, *filled diamond* TBF beads, *opened circle* H_2O_2–TBP, *filled circle* H_2O_2–TBP beads, *opened triangle* H_2O_2–TBF, *filled triangle* H_2O_2–TBF beads

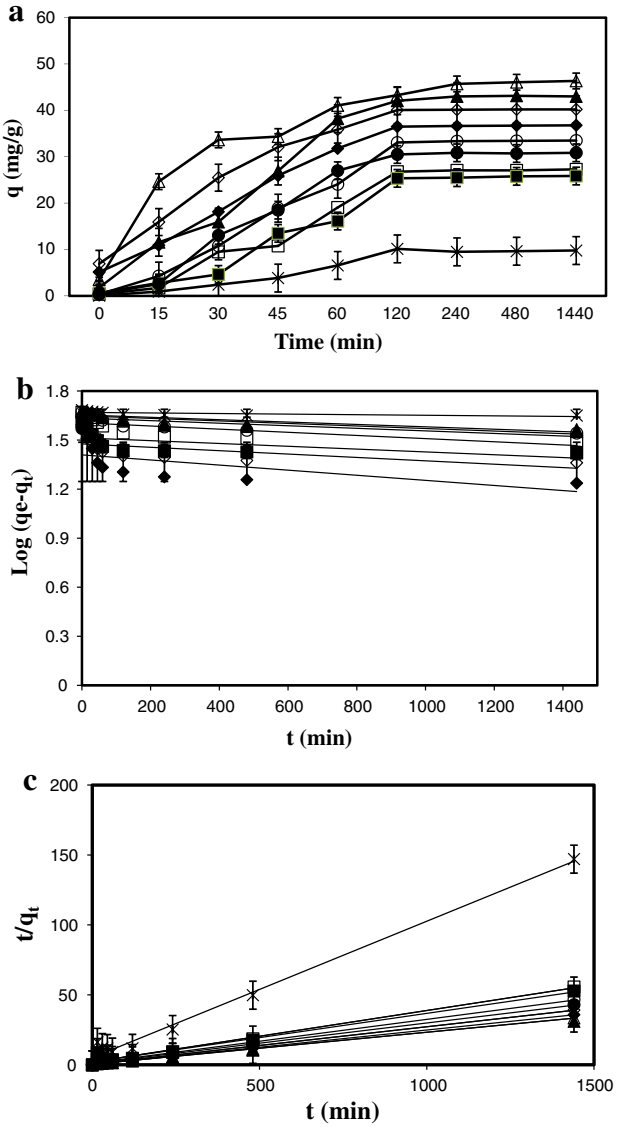

Fig. 3 **a** Effect of contact time, **b** first-order and **c** second-order plots of biosorption kinetics of Reactive Orange 122 by *T. bispinosa*'s peel and fruit. *Times symbol* PVA-alginate, *opened square* TBP, *filled square* TBP beads, *opened diamond* TBF, *filled diamond* TBF beads, *opened circle* H_2O_2–TBP, *filled circle* H_2O_2–TBP beads, *opened triangle* H_2O_2–TBF, *filled triangle* H_2O_2–TBF beads

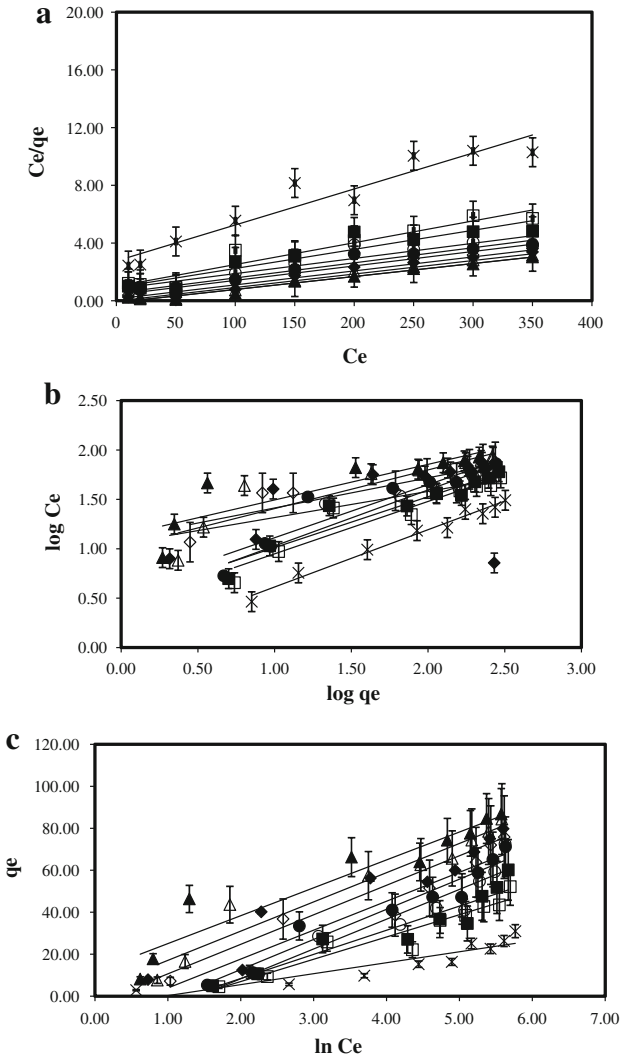

Fig. 4 Isotherm models **a** linearized Langmuir, **b** linearized Freundlich and **c** linearized Temkin for Reactive Orange 122 by *T. bispinosa*'s peel and fruit. *Times symbol* PVA-alginate, *opened square* TBP, *filled square* TBP beads, *opened diamond* TBF, *filled diamond* TBF beads, *opened circle* H_2O_2–TBP, *filled circle* H_2O_2–TBP beads, *opened triangle* H_2O_2–TBF, *filled triangle* H_2O_2–TBF beads

equilibrium concentrations of dye solution; V represents volume of dye solution (L), and M (g) stands for sorbent amount.The quantity of desorbed dye was computed from the following equation:

$$q_d = \frac{(C_e - C_d)}{M} \quad (3)$$

where q_d (mg g^{-1}) is the quantity of desorbed dye, C_e represents dye concentration before desorption, and C_d is the concentration of dye after desorption.

Statistical analysis

All the experiments were conducted in triplicate to minimize the handling error. The error bars in Figs. 2, 3, 4 and

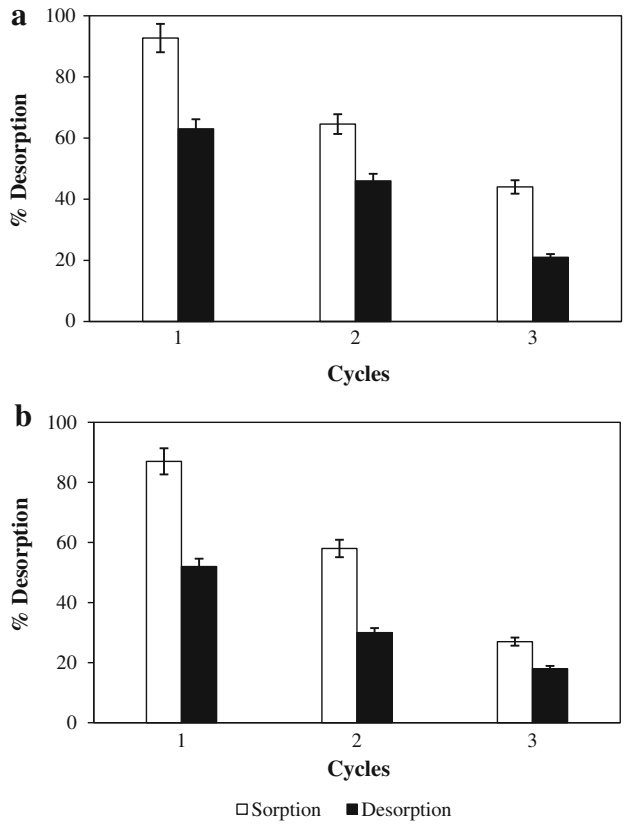

Fig. 5 Sorption–desorption cycles of **a** H_2O_2–TBF and **b** H_2O_2–TBF beads for RO 122

5 represent standard error. Linear regression was applied over data.

Results and discussion

Maximum wavelength (λ) determination for RO 122

λ (Lambda) is the wavelength at which the maximum fraction of light is absorbed by a solution. λ is a Greek letter that is used as the symbol for wavelength. The absorbance measurement was obtained using the PG-T 60 Spectrophotometer. Calibration curve of RO 122 was recorded over the wavelength range of 400–800 nm as shown in Fig. 1b. The maximum absorbance of the Reactive Orange C2RL 122 (RO 122) was 500 nm.

Palanisamy et al. (2012) reported the wavelength of maximum absorption (λ_{max}) for Reactive Red 195 at 543 nm by UV–Vis spectrophotometer in their study "Polymer Composite-A Potential Biomaterial for the Removal of Reactive Dye."

Khatib et al. (2012) determined characteristic absorbance of methylene blue using a single-beam UV–Vis spectrophotometer (Model SPUV-19) at a wavelength of maximum absorbance at 660 nm in their study "Adsorption from aqueous solution onto natural and acid activated bentonite."

Effect of pH on the sorption of RO 122 by *T. bispinosa*'s peel and fruit

The variation in equilibrium uptake with different initial pH studied ranging from 1.0 to 6.0 keeping constant initial dye concentration at 50 mg L^{-1} and sorbent dose 0.1 g. Results were obtained in the form of absorbance using UV–Vis spectrophotometer.

Figure 2a shows that maximum sorption of RO 122 by PVA-alginate, TBP, TBP beads, TBF, TBF beads, H_2O_2–TBP, H_2O_2–TBP beads, H_2O_2–TBF and H_2O_2–TBF beads were found to be extremely pH depended. The maximum sorption occurred at pH 1.0 and then declined sharply by the further increase in pH.

The effect of pH on dye sorption was explained by electrostatic force of attraction between *T. bispinosa* and dye molecules. Reactive dyes are mainly azo-based chromophores having different types of reactive groups, which interact with the active groups on the cell surface of biosorbent. More accurately, the RO 122 is bifunctional, monochlorotriazine and vinyl sulfone. Reactive dye release colored anion in the aqueous solution. So, maximum removal obtained at acidic environment due to electrostatic force of attraction between positively charged active group present on biosorbent surface and these negatively charged dye anion in the solution. At lower pH, more hydrogen ions present in the solution that act as bridging ligand between dye molecule and *T. bispinosa*'s cell surface. As the pH increase, OH^- ion replaces the H^+ concentration that induced electrostatic repulsion due to changed chemistry of biosorbent active group and sharp decline was observed in sorption process (Mezohegyi et al. 2012; Wang et al. 2012).

Proposed sorption mechanisms regarding pH

Any sorbent follows two type of mechanisms for the pH effect on sorption of dyes: (a) force of interaction among protonated/deprotonated groups of adsorbents with dye and (b) the chemical reaction between the sorbate and the sorbent. Main active sites for binding of anionic dyes by TB are the hydroxyl groups on the surface of TB.

For anionic dye (RO 122), main mechanism involves surface interaction between the anionic dye and the acidic phenolic hydroxyl (OH_2^+) groups in sorbents. At acidic pH,

$$TB{-}OH + H_3O^+ \rightarrow TB{-}OH_2^+ + H_2O \quad (4)$$

where TB stands for the surface of sorbent. The association of dye anion and positively charged surface of sorbent may be expressed as

$$Dye^- + TB{-}OH_2^+ \rightarrow TB{-}OH_2^+Dye^- \quad (5)$$

With increases in pH value, hydroxyl groups (OH^-) increase resulting in repulsion between anionic dye and sorbent surface; hence, a significant decrease in dye sorption occurs at higher pH. At basic pH,

$$TB{-}OH + HO^- \rightarrow TB{-}O^- + H_2O \quad (6)$$

Repulsion between the negatively charged surface of adsorbent and anionic dye may be expressed as (Seey and Kassim 2012).

$$TB{-}O^- + Dye^- \rightarrow TB{-}O^-/Dye^- \quad (7)$$

Similar observation has been reported in published literatures, where reactive dye sorption decreases as the pH increases. Janos et al. (2003) worked on removing anionic and cationic dyes on ash. They found out the cationic dye removal increases with rising pH; however, by pH reduction, the ionic dyes removal increase.

Effect of dye concentration on the sorption by *T. bispinosa*'s peel and fruit

Reactive dyes are being used extensively in textile industries and their effluent directly poured into water stream without treatment. That's why waste water contains higher concentration of reactive dyes (Aksu and Tezer 2005; Caner et al. 2009). Effect of dye initial concentration of RO 122 by free, immobilized and H_2O_2-treated sorbent at pH: 1, sorbent dose, 0.1 g/50 mL (C_i: 10, 20, 25, 50, 100, 150, 200, 250, 300 and 350 mg L^{-1}), particle size: 0.25 mm, shaking speed: 100 rpm, was investigated.

Figure 2b shows the uptake capacity versus dye initial concentration. Figure 2b shows that among all the sorbent H_2O_2–TBF exhibited maximum sorption increased from 8.14 to 86.80 (mg g^{-1}) for RO 122. As dye initial concentration number of collisions between dye anions and sorbent increases, this enhances the sorption process (Binupriya et al. 2010).

The percentage removal of dye was found to be decreasing with the increase in initial dye concentration. % removal was decreased from 81.40 to 24.80 % by H_2O_2–TBF. The sorbent has a fixed number of binding sites that become saturated over a definite concentration. At low dye concentrations, the ratio of binding sites present on sorbent to the total dye molecules in the solution is higher, and hence, all the anionic dye molecules may attach with the active functional groups such as –COOH, –OH, –CO, $–NH_3$ on the surface of the *T. bispinosa* and removed from the solution. On the other hand, by increasing dye concentrations, the number of active sorption sites is not sufficient to lodge all the dye molecules. Consequently, the sorption approached saturation stage and hence decreased in % removal observed. Similar behaviors were reported by Hameed et al. (2009) for the sorption of Reactive Red 120 using palm oil as industry waste and the sorption of Reactive Orange by activated carbons prepared from sugarcane bagasse pith by Amin (2008).

These studies demonstrated that *T. bispinosa* is excellent sorbent even at higher concentration of dye.

Effect of contact time on the sorption of RO 122 by *T. bispinosa*'s peel and fruit

Deployment of the biomass for practical application can be done successfully by studying relationship of sorption with contact time. For establishing an appropriate contact time between the biomass (0.1 g) and dye solution (50 mL), sorption capacity of *T. bispinosa*'s peel and fruit was measured as a function of time (0–1,440 min). Figure 3a shows the effect of contact time on the sorption of RO 122. Sorption process was rapid in the first 30 min and attained equilibrium in 120 min, further increase in contact time did not enhance the adsorption. Within 90 min, H_2O_2–TBF beads showed 52.28 % removal for RO 122.

Sorption process occurs in two phases, initial phase (rapid phase) and final phase (equilibrated phase). The initial rapid adsorption may be attributed to the presence of positive charge on the biosorbent surface, which developed an interaction with negatively charged dye. However, after a lapse of time, the available sorption sites were reduced and the occupied sorption sites become saturated. Then, the biosorption began to slow down due to slow movement of dye molecule into the interior bulk of the biosorbent of solute into the interior of the adsorbent (Hii et al. 2011; Sreelatha et al. 2011; Seey and Kassim 2012). Therefore,

120 min was deemed sufficient to establish equilibrium in subsequent experiments.

Abassi and Asl (2009) used grapefruit peel for RB19 removal. The equilibrium condition was achieved within 45 min.

Kinetic models

The study of kinetics is essential for the exploration of solute uptake rate, which controls the retention time of sorption process. The results would be of undeniable importance for the optimization process in industry. In the present study, the kinetics of the reactive dye was carried out at different temperatures to understand the behavior of TBP and TBF.

Pseudo-first order

Pseudo-first order kinetic model assumes that "metal sorption process is first order in nature as it is only dependent on the number of metal ions present at the specific time in the solution". The pseudo-first-order equation is shown below (Salvestrini et al. 2010):

$$\log(q_e - q_t) = \log q_e - K_1 t \div 2.303 \quad (11)$$

where K_1 is the rate constant of the pseudo-first-order sorption. The nonlinear plot of Log $(q_e - q_t)$ versus t showed non-significant regression coefficient. Results in Table 1 and Fig. 3b show that the adsorption data could not be fitted by this model for RO 122. This indicates that pseudo-first-order kinetics might be insufficient to interpret the mechanism of reactive dyes sorption.

Nanthakumar et al. (2009) studied biosorption equilibria and kinetics of Reactive blue 140 using dead fungal biomass of *Aspergillus niger*. They found that R^2 values for the pseudo-first-order kinetic plots were lower than those for pseudo-second-order kinetic plots.

Pseudo-second order

Pseudo-second order is also based upon the sorption capacity of the sorbent material. The pseudo-second-order equation can be written as (Salvestrini et al. 2010):

$$\frac{t}{q_t} = \frac{1}{K_2 q_e^2} + \frac{1}{q_e} \times t \quad (12)$$

where K_2 is the rate constant of the pseudo-second-order sorption.

The plot of t/q_t versus t showed a linear relationship with high regression coefficient as compared to pseudo-first-order model. Kinetics parameters are tabulated in Table 1 calculated from Fig. 3c. Data showed that there is excellent compliance between pseudo-second-order theoretical and experimental q_e values. The correlation coefficient for the pseudo-second-order model is significantly higher than that of pseudo-first-order model.

Sorption isothermal modeling

Equilibrium data, generally known as sorption isotherms, are basic requirements for the design of sorption mechanism. The isotherm indicates how the molecules distribute between the liquid and solid phases when sorption reaches the equilibrium. In most studies related to dye adsorption, three well-known isotherms predominate that are studied below.

Langmuir isotherm model

Langmuir isotherm model is valid for monolayer sorption process onto a surface with a finite number of energetically equivalent identical sites. The linear form of Langmuir's isotherm model is given by the following equation (Safa and Bhatti 2011):

$$\frac{C_e}{q_e} = \frac{1}{X_m K_L} + \frac{C_e}{X_m} \quad (8)$$

where q_e (mg g^{-1}) is equilibrium sorption capacity, and C_e (mg L^{-1}) is dye equilibrium concentration. X_m (mg g^{-1}) is sorption capacity. K_L (dm^3 g^{-1}) is Langmuir constant termed as apparent energy of adsorption. Linear plots are obtained when C_e/q_e is plotted against C_e over the entire concentration range of dye by free, immobilized and H_2O_2-treated sorbents and shown in Fig. 4a.

The value of correlation coefficients showed that Langmuir equation was the best fitted for TBP beads (0.926), TBF (0.962), TBF beads (0.902), H_2O_2–TBP (0.939), H_2O_2–TBF (0.977) and H_2O_2–TBF beads(0.979) for RO 122 dye as shown in Table 2. The sorption isotherms exhibit Langmuir behavior for some sorbents, which indicates a monolayer biosorption.

Freundlich isotherm model

The Freundlich isotherm assumes that sorption takes place on heterogeneous surfaces and the sorption capacity depends on the concentration of dye at equilibrium. The

Table 1 Comparison between pseudo-first-order and pseudo-second-order kinetic models for Reactive Orange 122

Sorbent	First order			Second order			q_{exp} (mg g^{-1})
	q_e (mg g^{-1})	K_1 (min^{-1})	R^2	q_e (mg g^{-1})	K_2 (min^{-1})	R^2	
PVA-alginate	43.75	0.00012	0.320	10.31	0.0018	0.988	10.14
TBP	29.79	0.00046	0.311	29.41	0.0056	0.976	27.29
TBP beads	32.36	0.00092	0.340	27.78	0.00066	0.987	25.86
TBF	29.51	0.0014	0.388	38.46	0.0017	0.999	40.21
TBF bead	31.33	0.003	0.338	35.71	0.00078	0.994	36.79
H_2O_2–TBP	34.21	0.00023	0.308	41.67	0.0026	0.999	33.50
H_2O_2–TBP beads	36.89	0.0018	0.381	32.26	0.0008	0.987	30.86
H_2O_2–TBF	32.21	0.0016	0.240	47.62	0.09	0.999	46.36
H_2O_2–TBF beads	12.88	0.00023	0.057	45.45	0.011	0.998	43.00

Table 2 Equilibrium isotherm parameters for Reactive Orange 122 *T. bispinosa*'s peel and fruit

Sorbent	Langmuir isotherm			Freundlich isotherm			Temkin isotherm			q_{exp} (mg g^{-1})
	X_m (mg g^{-1})	R^2	K_L (mg g^{-1})	q_e (mg g^{-1})	K_F (mg g^{-1})	R^2	b_T (KJ mol^{-1})	K_T (dm^3 g^{-1})	R^2	
PVA-alginate	40.00	0.917	0.0091	30.38	1.0789	0.98	475.36	0.00744	0.828	31
TBP	76.92	0.881	0.0143	48.25	3.141	0.903	215.44	4×10^{-07}	0.889	60.2
TBP beads	66.66	0.926	0.0151	53.6	2.618	0.897	233.73	6×10^{-07}	0.915	52.2
TBF	111.11	0.962	0.072	49.42	11.272	0.231	176.21	0.03341	0.917	79.8
TBF bead	100.00	0.902	0.025	70.06	12.794	0.803	179.79	5×10^{-05}	0.882	75.8
H_2O_2–TBP	100.00	0.939	0.0189	76.85	3.758	0.872	172.65	1×10^{-07}	0.94	71.2
H_2O_2–TBP beads	100.00	0.882	0.0121	69.95	2.897	0.916	174.72	2×10^{-09}	0.906	72.6
H_2O_2–TBF	111.11	0.977	0.075	100.99	13.58	0.75	186.42	12.54	0.91	84.8
H_2O_2–TBF beads	111.11	0.979	0.043	91.8	10.35	0.827	177.99	23.3127	0.94	84.4

Freundlich equation is an empirical equation, and its linearized form can be given as (Zawani et al. 2009):

$$\log q_e = \log K_F + \frac{1}{n}\log C_e \quad (9)$$

where K_F and $1/n$ are the Freundlich constants, they are related to the adsorption capacity and intensity, respectively. The Freundlich constants K_F and $1/n$ can be calculated from the slope and intercept of the linear plot, with log q_e versus log C_e as shown in Fig. 4b.

Table 2 shows the result of free, immobilized and pretreated TBP and TPF. These results depicted that Freundlich isotherm was best fitted to PVA-alginate (0.98), TBP (0.903), H_2O_2–TBP beads (0.916) for RO 122 in comparison with the Langmuir model.

The model parameters and regression coefficient obtained for Freundlich isotherm showed a significant lower correlation with the experimental data compared to Langmuir model.

Temkin isotherm

The Temkin isotherm model (Temkin and Pyzhev 1940) explains an equal division of binding energies for the number of exchanging sites on the sorbent surface. The Temkin equation has the following form.

$$q = \frac{RT}{b_T}\ln K_T + \frac{RT}{b_T}\ln c \quad (10)$$

where b_T is the heat of sorption (kJ mol^{-1}), K_T is the

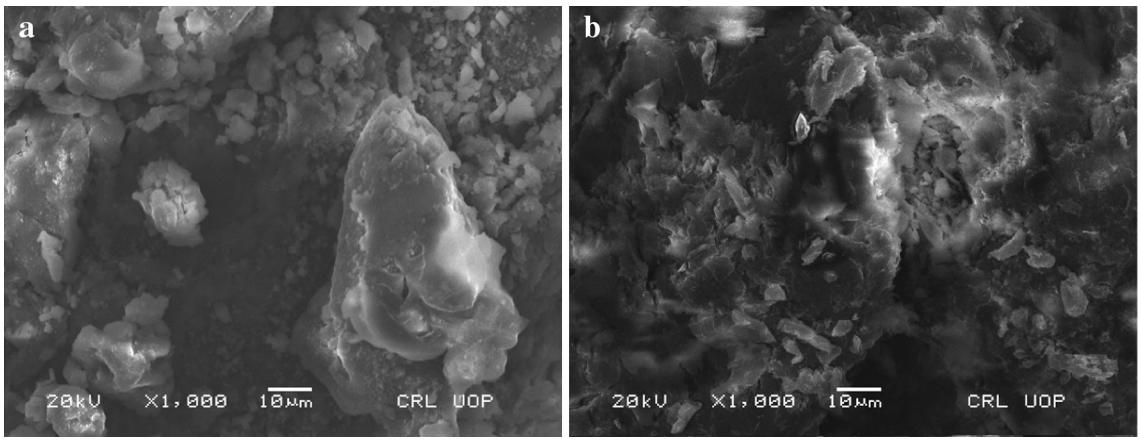

Fig. 6 Scanning electron micrograph (SEM) of **a** TBF before sorption, **b** TBF after sorption

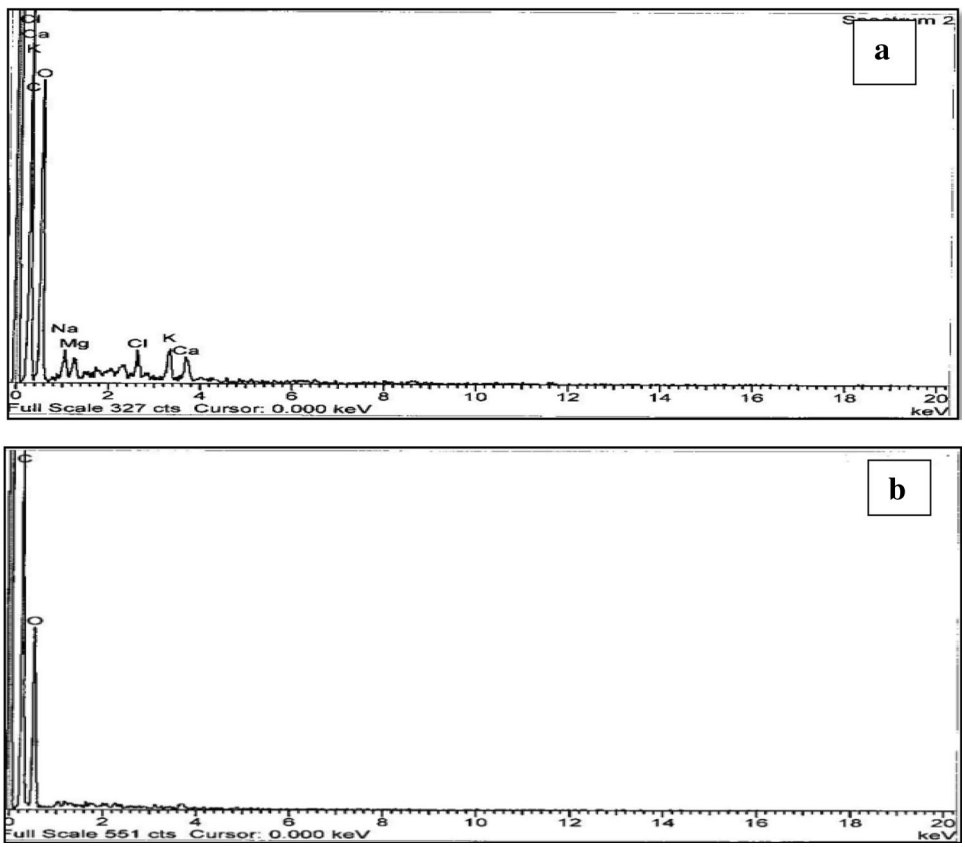

Fig. 7 EDX spectrum for **a** TBF before sorption, **b** TBF after sorption

intensity of sorption ($dm^3\ g^{-1}$), R is the Universal gas constant, and T is the absolute temperature.

Table 2 and Fig. 4c show that Temkin model is not well fitted the adsorption process of RO 122 in comparison with the Langmuir model and Freundlich model.

Thermodynamic parameter

Thermodynamic deliberation for sorption process is essential to find out whether the process is spontaneous or not. ΔG° (change in Gibbs free energy) explains the

spontaneity of a reaction. Langmuir isotherm equation was applied to calculate the thermodynamic parameters as follows (Baseri et al. 2012):

$$\Delta G^{\circ} = -RT \ln K_c \quad (25)$$

where K_c represents equilibrium constant (q_e/C_e), T stands for temperature, and R is the gas constant. E_P is the equilibrium parameter defined as:

$$E_P = 1/(1 + bC_i) \quad (26)$$

The negative values of ΔG° confirm the spontaneity and feasibility of sorption process for RO 122 onto *T. bispinosa*. E_P values greater than zero and less than unity ($0 < E_P < 1$) for RO 122 dye sorption indicates that Langmuir isotherms is favorable for the applicability.

Desorption

Desorption studies helps to evaluate the mechanism of sorption and upturn of sorbate and sorbent. The effectiveness of dye adsorption and desorption from a solution was determined based on changing in the concentration of dye left in the solution. Figure 5 shows that cyclic sorption/desorption was carried out for RO 122, by H_2O_2–TBF and H_2O_2–TBF beads using 0.01 N NaOH reagent for desorption.

The obtained results indicated that the highest efficiency of % desorption was 62.72 in first cycle that decreased to 20.66 in third cycle by H_2O_2–TBF, while H_2O_2–TBF beads showed 51.71–18.36 % desorption for RO 122. This demonstrated the effectiveness of regeneration of H_2O_2–TBF higher than H_2O_2–TBF bead.

With the increase of repeated cycle, the rates of adsorption and desorption are decreased slightly. The quantity of adsorbed dye was very high in first two cycles as compared to the quantity of desorbed dye, whereas the effectiveness of both sorption and desorption was observed to decrease significantly in third cycle (Fig. 5). The reduction in the number of feasible sorption/desorption cycles was due to the depletion of active sites of the sorbent being occupied by the dye.

Filipkowska and Rodziewicz (2011) analyzed cyclic sorption and desorption of four reactive dyes: Reactive Yellow 84, Reactive Red 11, Reactive Black 5 and Reactive Black 8 onto chitosan beads. They investigated the number of feasible sorption/desorption cycles ranged from 6 to 3 and found number of cycles depend on the type of dye tested.

Scanning electron microscopy (SEM) analysis

Scanning electron microscope is a type of electron microscope capable of creating higher magnified images of sample surface. The production of magnified images is due to using electrons instead of light waves, which also provide SEM images with three-dimensional characteristic appearance of sample. The size, shape, porosity and arrangement of the particles making up the object present over the surface of sorbent can be well studied by SEM.

The surface image before and after the sorption phenomenon was taken to observe the morphology of TBF as shown in Fig. 6a, b.

From SEM images, it is clear that pores within the *T. bispinosa* particles were heterogeneous with the large microspores and inter-particle cavities. Original *T. bispinosa* showed the presence of significant number of pores providing a suitable position for dyes to be adsorbed. It is observed that the pore size of raw is significantly higher.

SEM images after RO 122 dye adsorption demonstrated that the pores and cavities of adsorbent were efficiently packed with dyes. The surface and pores of *T. bispinosa* were coated with dyes causing smoother surface and minimizing pore size. It is concluded that the pore size changed with the incorporation or sorption of the dye molecules.

EDX analysis (characterization of adsorbent)

The EDX analysis of TBF before and after sorption with RO 122 is presented in Fig. 7a–b. The EDX results demonstrated Ca, K and Na, Mg, C and O are the main components of *T. bispinosa*. Presence of these elements could affect the adsorption mechanism through ionic exchange interactions. Decrease in peaks height may be related to ionization degree of dye molecules and relevance functional groups on *T. bispinosa* surface. Also, this phenomenon might be associated with electrostatic force of interactions between positive and negative charges of RO 122 and *T. bispinosa* surface.

Conclusion

Dye effluent due to rapid industrialization is one of the most significant problems of Pakistan and all over the world. For this context, *T. bispinosa*, a new cost-effective biosorbent was evaluated. Maximum uptake was observed at pH 1.0. At low pH value, H^+ acts as bridging ligand and highest electrostatic force of attraction was there for the maximum removal of reactive dyes. By increasing dye concentration from 10 to 350, q (mg g^{-1}) increased. The sorption rate was rapid in first

30 min, and equilibrium was established in 120 min. It was observed that best model was pseudo-second order, with correlation coefficient in the range of 0.987–1.00. The Langmuir model effectively described the biosorption data. Regeneration of the sorbent was done by performing desorption cycles, which made the method environment-friendly and more economical. For the purpose of characterization of sorbent, SEM and EDX analysis were performed.

Acknowledgments Authors are thankful to the Chairperson, Department of Chemistry and Biochemistry, University of Agriculture Faisalabad, Pakistan, for providing research facilities.

References

Abassi M, Asl NR (2009) Removal of hazardous reactive blue 19 dye from aqueous solutions by agricultural waste. J Iran Chem Soc 2:221–230

Aksu ZS, Agatay SC (2006) Investigation of biosorption of Gemazol Turquoise blue-G reactive dye by dried *Rhizopus arrhizus* in batch and continuous systems. Sep Purif Technol 48:24–35

Aksu Z, Balibek E (2010) Effect of salinity on metal-complex dye biosorption by *Rhizopus arrhizus*. J Environ Manage 91:1546–1555

Aksu ZM, Tezer S (2005) Biosorption of reactive dyes on the green alga *Chlorella vulgaris*. Process Biochem 40:1347–1361

Amin NK (2008) Removal of reactive dye from aqueous solutions by adsorption onto activated carbons prepared from sugarcane bagasse pith. Desalination 223(1–3):152–161

Asgher M, Bhatti HN (2012) Removal of reactive blue 19 and reactive blue 49 textile dyes by citrus waste biomass from aqueous solution: equilibrium and kinetic study. Can J Chem Eng 90(2):412–419

Bai RS, Abraham TE (2003) Studies on chromium (VI) adsorption desorption using immobilized fungal biomass. Bioresour Technol 87:17–26

Baseri JR, Palanisamy PN, Sivakumar P (2012) Adsorption of reactive dye by a novel activated carbon prepared from *Thevetia peruviana*. Int J Chem Res 3(2):36–41

Beolchini F, Pagnanelli F, Toro L, Veglio F (2003) Biosorption of copper by *Sphaerotilus natans* immobilized in polysulfone matrix: equilibrium and kinetics analysis. Hydrometallurgy 70:101–112

Bhatti HN, Bajwa II, Hanif MA, Bukhari IH (2010) Removal of lead and cobalt using lignocellulosic fiber derived from *Citrus reticulate* waste biomass. Korean J Chem Eng 27:218–227

Binupriya AR, Sathishkumar M, Ku CS, Yun S (2010) Sequestration of reactive blue 4 by free and immobilized *Bacillus subtilis* cells and its extracellular polysaccharides. Colloids Surf B Biointerfaces 76:179–185

Caner N, Kiran I, Ilhan S, Iscen CF (2009) Isotherm and kinetic studies of Burazol Blue ED dye biosorption by dried anaerobic sludge. J Hazard Mater 165:279–284

Crini G (2006) Non conventional low cost adsorbents for dye removal: a review. Bioresour Technol 97:1061–1085

Deniz F, Karaman S (2011) Removal of Basic Red 46 dye from aqueous solution by pine tree leaves. Chem Eng J 170:67–74

Fernandez ME, Nunell GV, Bonelli PR, Cukierman AL (2008) Batch and dynamic biosorption of basic dyes from binary solutions by alkaline-treated cypress cone chips. Bioresour Technol 99:7971–7975

Filipkowska U, Rodziewicz J (2011) Cyclic sorption and desorption of reactive dyes onto chitosan beads. Prog Chem Appl Chitin 1051:71–78

Gadd GM (2009) Biosorption: critical review of scientific rationale, environmental importance and significance for pollution treatment. J Chem Technol Biotechnol 84:13–28

Hameed BH, Ahmad AA, Aziz N (2009) Adsorption of reactive dye on palm-oil industry waste: equilibrium, kinetic and thermodynamic studies. Desalination 247(1–3):551–560

Handan U (2011) Equilibrium, thermodynamic and kinetics of reactive black 5 biosorption on loquat (*Eriobotrya japonica*) seed. Sci Res Essays 6(19):4113–4124

Hii SL, Estrop LL, Wong CL (2011) Adsorption of reactive blue 4 onto the chemically modified red seaweed *Amphiroa foliacea*: equilibrium, kinetics and modeling studies. Int J Phys Sci 6(31):7171–7182

Iqbal DMK, Ahmed S, Alam DS, Ahmed DM (2011) Sustainable management of textile waste water of Pakistan. World Water Day April 96–105

Janos P, Buchtova H, Ryznarova M (2003) Sorption of dyes from aqueous solutions onto fly ash. Water Res 37(20):4938–4944

Ju DJ, Byun IG, Park JJ, Lee CH, Ahn GH, Park TJ (2008) Biosorption of a reactive dye (Rhodamine-B) from an aqueous solution using dried biomass of activated sludge. Bioresour Technol 99:7971–7975

Junxiong C, Longzhe C, Yanxin W, Chengfu L (2009) Effect of functional groups on sludge for biosorption of reactive dyes. J Environ Sci 21:534–538

Khatib LA, Fraige F, Hwaiti MA, Khashman OA (2012) Adsorption from aqueous solution onto natural and acid activated bentonite. Am J Environ Sci 8(5):510–522

Mao J, Won SW, Vijayaraghavan K, Yun YS (2010) Immobilized citric acid treated bacterial biosorbents for the removal of cationic pollutants. Chem Eng J 162(2):662–668

Mezohegyi G, Zee FP, Font J, Fortuny A, Fabregat A (2012) Towards advanced aqueous dye removal processes: a short review on the versatile role of activated carbon. J Environ Manag 102:148–164

Mondal S (2008) Methods of dye removal from dye house effluent: an overview. Environ Eng Sci 25:383–396

Murugesan K, Nam IH, Kim YM, Chang YS (2006) Decolorization of reactive dyes by a thermostable laccase produced by Ganoderma lucidum in solid state culture. SESE 31:790–784

Nanthakumar K, Karthikeyan K, Lakshmanaperumalsamy P (2009) Investigation on biosorption of reactive blue 140 by dead biomass of *Aspergillus niger* HM11: kinetics and isotherm studies. Glob J Biotechnol Biochem 4(2):169–178

Oei BC, Ibrahim S, Wang S, Ang HM (2009) Surfactants modified barley straw for removal of acid and reactive dyes from aqueous solution. Bioresour Technol 100:4292–4295

Palanisamy PN, Agalya A, Sivakumar P (2012) Polymer composite—a potential biomaterial for the removal of reactive dye. J Chem 9(4):1823–1834

Ponnusami V, Krithika V, Madhuram R, Srivastava SN (2007) Biosorption of reactive dye using acid-treated rice husk: factorial design analysis. J Hazard Mater 142(1–2):397–403

Sadaf S, Bhatti HN (2011) Biosorption of Foron turquoise SBLN using mixed biomass of white rot fungi from synthetic effluents. Afr J Biotechnol 10(62):13548–13554

Sadettin S, Donmez G (2006) Bioaccumulation of reactive dyes by *thermophilic cyanobacteria*. Process Biochem 41:836–841

Safa Y, Bhatti HN (2011) Adsorptive removal of direct dyes by low cost rice husk: effect of treatments and modifications. Afr J Biotechnol 10(16):3128–3142

Salvestrini S, Sagliano P, Iovino P, Capasso S, Colella C (2010) Atrazine adsorption by acid-activated zeolite-rich tuffs. Appl Clay Sci 49:330–335

Seey TL, Kassim MJNM (2012) Characterization of mangrove bark adsorbent and its application in the removal of textile dyes from aqueous solution. J Appl Phytotechnol Environ Sanit 1(3):121–130

Sreelatha G, Ageetha V, Parmar J, Padmaja P (2011) Equilibrium and kinetic studies on reactive dye adsorption using palm shell powder (an agrowaste) and chitosan. Am Chem Soc 56(1):35–42

Temkin MJ, Pyzhev V (1940) Recent modification to Langmuir isotherm. Acta Physiochimica USSR 12:217–222

Vijayaraghavan K, Yun YS (2007) Chemical modification and immobilization of *Corynebacterium glutamicum* for biosorption of reactive black 5 from aqueous solution. Ind Eng Chem Res 46:608–617

Vijayaraghavan K, Lee MW, Yun YS (2008) A new approach to study the decolorization of complex reactive dye bath effluent by biosorption technique. Bioresour Technol 99:5778–5785

Wang H, Shen Y, Shen C, Wen Y, Li H (2012) Enhanced adsorption of dye on magnetic Fe_3O_4 via HCl-assisted sonication pretreatment. Desalination 284:122–127

Yesilada O, Asma D, Cing S (2003) Decolorization of textile dyes by fungal pellets. Process Biochem 38:933–938

Zawani Z, Chuah AL, Choong TSY (2009) Equilibrium, kinetics and thermodynamic studies: adsorption of Remazol black 5 on the palm kernel shell activated carbon (PKS-AC). Eur J Sci Res 37(1):63–71

Zhang D (2013) Synergetic effects of Cu_2O photocatalyst with Titania and enhanced photoactivity under visible irradiation. Acta Chim Slov 6(1):141–149